Langmuir
Article
pubs.acs.org/Langmuir

Sensing by Means of Nonlinear Optics with Functionalized GaAs/AlGaAs Photonic Crystals

Elias Estephan,[†] Daniele Bajoni,[§] Marie-belle Saab,[†] Thierry Cloitre,[†] Roger Aulombard,[†] Christian Larroque,[‡] Lucio Claudio Andreani,[⊥] Marco Liscidini,[⊥] Andrea Marco Malvezzi,[§] and Csilla Gergely*,[†]

[†]*Groupe d'Etude des Semi-conducteurs, UMR 5650, CNRS-Université Montpellier 2, 34095 Montpellier Cedex 5, France,* [‡]*IRCM/INSERM896, Centre Régional de Lutte contre le Cancer Val d'Aurelle-Paul Lamarque, Université Montpellier 1, 34298 Montpellier, France,* [§]*CNISM and Dipartimento di Elettronica, Universitá di Pavia, Via Ferrata 1, I-27100 Pavia, Italy, and* [⊥]*CNISM and Dipartimento di Fisica "A. Volta", Università di Pavia, Via Bassi 6, I-27100 Pavia, Italy*

Received January 7, 2010. Revised Manuscript Received March 4, 2010

We report on specific functionalization of GaAs/AlGaAs photonic structures for molecular sensing via the optical second harmonic generation signal in the visible range exhibited by these nanostructures. Functionalization has been achieved by peptides selected by the phage display technology, revealing specific recognition for semiconducting surfaces. These small peptides when biotinylated serve for controlled placement of biotin onto the substrate to capture then streptavidin. Functionalization (with biotinylated peptide) and molecular recognition (of streptavidin) events both result in enhancing the nonlinear optical response of the samples. Adsorption and infiltration of biomolecules into the GaAs/AlGaAs photonic structure were monitored by atomic force and scanning electron microscopy combined with Energy Dispersive X-ray spectroscopy. We demonstrate that once functionalized with specific peptides, photonic structures could be used as miniature biosensors down to femtomolar detection sensitivity, by monitoring changes in the second harmonic signal when molecules are captured. Our results prove the outstanding sensitivity of the nonlinear approach in biosensing with photonic crystal waveguides as compared to linear absorption techniques on the same samples. The present work is expected to pioneer development of a new class of extremely small affinity-based biosensors with high sensitivity and demonstrates that photonic structures support device functionality that includes strongly confined and localized nonlinear radiation emission and detection processes.

Introduction

The interface between biological molecules and inorganic surfaces yet still underexplored is a key issue for nanobiotechnologies exploiting biomolecular recognition and self-assembly capabilities for integrating advanced materials into medicine and electronics.[1] In particular, the efficiency of biosensor devices is directly determined by the interfacial adsorption of biomolecules. Detection often requires fluorescent labeling of proteins or use of a metal surface for sensing via surface plasmon resonance.[2] In both cases there is a risk of structural modification or denaturation of the protein when labeling occurs or when there is contact with the metal surface, respectively. Thus functionalization is an important issue in developing affinity-based optical biosensors. The inconveniences of the mainstream optical biosensor methods are the required large sensing area and the substrate-dependent binding of molecules driven by unspecific interactions, which give rise to serious limitations in sensing performances and the detection limit. Strong research interest has been devoted in recent years toward miniaturization of the sensing surface (especially through the use of surface plasmons[3,4]) and the capability of single or few molecule detection (via surface plasmons or high-Q optical cavities).[3−6] Miniaturization, maintaining at the same time a large sensing area by assuring high specificity of the sensing surface, is however an important challenge of nowadays research in biosensing. Emphasis should be given on developing alternative sensing methods and new sensing substrates presenting high binding selectivity and sensitivity for biological molecules.

In this work we report on the elaboration of a functionalized nanostructured semiconductor substrate for biosensing applications. In this case there is the possibility of a surface functionalization via nanometer-sized adhesion peptides coupled at the same time to a wider range of detection possibilities that originate from the presence of a transparency region. Moreover, spatial modulation of the material may give rise to regions of enhanced fields that in turn may be instrumental in the detection of small variations of the structure itself caused by the surface adhesion of molecules either by linear or nonlinear optical techniques.

Nonlinear optics has become a new and exciting area of research to probe and study biological molecules. Second harmonic generation (SHG) has been proven to be a powerful method for detection of biomolecules adsorbed on a surface and determining the orientation of their functional groups.[7,8] Even isotropic media originally producing no SH might be detected by nonlinear optics because at a surface the inversion

*Corresponding author. E-mail: Gergely@ges.univ-montp2.fr.

(1) Cunningham, B. T.; Li, P.; Lin, B.; Pepper, J. *Sens., Actuators B* **2002**, *81*, 316–328.
(2) Schuster, S. C.; Swanson, R. V.; Alex, L. A.; Bourret, R. B.; Simon, M. I. *Nature* **1993**, *365*, 343–347.
(3) Cubukcu, E.; Zhang, S.; Park, Y. S.; Bartal, G.; Zhang, X. *Appl. Phys. Lett.* **2009**, *95*, 043113–043115.
(4) De Angelis, F.; Das, G.; Candeloro, P.; Patrini, M.; Galli, M.; Bek, A.; Lazzarino, M.; Maksymov, I.; Liberale, C.; Andreani, L. C.; Di Fabrizio, E. *Nat. Nanotechnol.* **2010**, *5*, 67–72.
(5) Nitkowski, A.; Chen, L.; Lipson, M. *Opt. Express* **2008**, *16*, 11930–11936.
(6) Armani, A. M.; Kulkarni, R. P.; Fraser, S. E.; Flagan, R. C.; Vahala, K. J. *Science* **2007**, *317*, 783–787.
(7) Chen, W.; Feller, M. B.; Shen, Y. R. *Phys. Rev. Lett.* **1989**, *63*, 2665–2668.
(8) Marowsky, G.; Lupke, G.; Steinhoff, R.; Chi, L. F.; Mobius, D. *Phys. Rev. B* **1990**, *41*, 4480–4483.

symmetry is necessarily broken and SH can appear. Hence, SH spectroscopy is an intrinsically surface-selective technique particularly suitable to monitor not only protein adsorption and protein−protein interactions but also conformational change of proteins[9,10] at interfaces.

Our objective is to exploit semiconductor structures for molecular detection by mean of nonlinear optics. Miniaturization and large sensing area is assured by photonic crystals (PhC). Photonic crystals are nanostructured materials in which the refractive index is periodically modulated: they are a widely used tool in solid state physics and photonics because they allow tuning the intensity and spatial distribution of photonic modes by changing the design parameters.[11] Photonic crystals can be easily integrated in semiconductor devices as they are generally obtained by patterning planar waveguides using well established top-down approaches.[12−14]

High specificity can be achieved by their proper functionalization with peptides that reveal specific recognition for semiconductor substrates.[15] Such peptides, produced by phage display technique, are used for controlled placement of biomolecules opening the way for producing user-tailored patterned hybrid materials for large-scale applications.[15−20] A new sensing method based on the signal enhancement and nonlinear optical response of PhCs can be encompassed owing to strongly confined and localized electromagnetic fields within these structures. Moreover, specific functionalization of PhC can lead to ordered arrays of a single variety of molecules, presenting all the advantages to constitute a biologically derived high-selectivity-based optical biosensor.

We report on the specific functionalization of a GaAs/AlGaAs photonic crystal structure with adhesion peptides for the GaAs (100) surface. The peptide produced by the phage display library presents a high affinity for the GaAs surface as demonstrated by our mass spectrometry (MS) measurements. The adsorption and correct infiltration of the biotinylated peptide into the GaAs/AlGaAs photonic crystal was checked by atomic force microscopy and scanning electron microscopy (SEM)−energy dispersive X-ray (EDX) spectroscopy. We demonstrate the capacity of detecting streptavidin molecules by monitoring changes in the SHG intensity when molecules are exposed and then captured by the biotinylated photonic surface.

Materials and Methods

GaAs Semi-insulating Substrate. The (100) GaAs samples are semi-insulating substrates grown by the liquid encapsulated Czochralki (LEC) method supplied by Sumitomo Ltd. (Japan). Before use the GaAs wafer was cleaved to $5 \times 5\ mm^2$ samples, and then carefully cleaned by successive treatments with trichloroethane, acetone, and methanol, rinsed in deionized water, and then dried with N_2. To remove the native oxide, just before functionalization, samples were treated with dilute HCl (HCl: H_2O = 1:10) for 2 min, then immersed in deionized water and nitrogen dried, according to protocols given in previous works.[15] The condition of the sample surface was monitored by atomic force microscopy (not shown).

Fabrication of the Photonic Structure. The photonic crystal samples have been obtained by electron beam lithography and were provided by the technological "nanostructuring platform" within the Network of Excellence (ePIXnet). The GaAs/$Al_{0.6}Ga_{0.4}As$ material was spin coated and baked in order to build a silica mask on top of it, using commercially available hydrogen silsesquioxane (HSQ). Electron beam lithography with polymethyl-methacrylate (PMMA) was used for the pattern definition. Reactive ion etching (RIE) with fluorine chemistry was used for transferring the pattern into the hard mask. Finally the sample was deeply etched using chemically assisted ion beam etching (CAIBE).[12]

Phage Display Method. The M13 bacteriophage library (Molecular Probes) was exposed to the GaAs semi-insulating substrate in phosphate-buffered saline solution containing 0.1% TWEEN-20 (PBST) after a previous cleaning and etching. After the samples were rocked for 1 h at room temperature, the surfaces were washed typically 10 times by PBST to rinse the unbound phages. In the next step, the bound phages were eluted from the surface: glycine-HCl (pH = 2.2) solution was added for 10 min and then they were transferred to a fresh tube and neutralized with Tris-HCL (pH = 9.1). The eluted phages were infected into *Escherichia coli* ER2738 host bacterial cells and thereby amplified. After three rounds of biopanning, monoclonal phage populations were selected and analyzed individually. Finally, 10 phages were recovered and amplified, followed by extraction and sequencing of their DNA that will define the sequence of the expressed peptide.

Functionalization of GaAs and MALDI-TOF/TOF Mass Spectrometry Analysis. The SVSVGMKPSPRP (P1) peptide was synthesized (MilleGen, France) with purity higher than 80%. After the steps of cleaning and deoxidation, the GaAs sample was incubated in 90 μM of peptide P1 (diluted in PBST) for 2 h, followed by a thorough rinsing step with deionized water to remove PBST and unbound and excess peptide. In the next step the matrix αCHCA (5 mg/mL α-cyano-4-hydroxycinnamic acid in a solvent composed of acetonitril/H_2O/trifluoroacetic acid (50/50/0.1%)) was added to the surface of the sample and then dried for crystallization. For matrix assisted laser desorption isonization (MALDI) studies, the GaAs samples were fixed to the MALDI plate via a conductor double-sided tape and then analyzed by a 4800 Plus MALDI-TOF/TOF proteomics analyzer (Applied Biosystems, Foster City, CA) in positive reflector ion mode using a 20 kV acceleration voltage. The YAG laser was operated at a 200 Hz firing rate with a wavelength of 355 nm. MS spectra were acquired for each measure using 1500 laser shots. Upon laser illumination and thanks to the matrix, the surface-bound peptide was positively charged, accelerated in the vacuum spectrometer chamber, detected, and characterized for its mass. The measured spectra were processed using the 4000 Series Explorer software (Applied Biosystems).

To identify the spectral line of the peptide, a reference dilution of P1 peptide was mixed with the matrix solution, and the resulting mixture was deposited onto the stainless steel sample plate. As control, the mass spectra obtained from the bare GaAs with the matrix alone was also recorded (data not shown).

Atomic Force Microscopy (AFM). AFM images were recorded in air, with an Asylum MFP-3D head and molecular force probe 3D controller (Asylum Research, Santa Barbara,

(9) Salafsky, J. S. *J. Chem. Phys.* **2006**, *125*, 1–7.
(10) Clarke, M. L.; Wang, J.; Chen, Z. *J. Phys. Chem. B* **2005**, *109*, 22027–22035.
(11) Joannopoulos, J. D.; Johnson, S. G.; Winn, J. N.; Meade, R. D. In *Photonic Crystals: Molding the Flow of Light*, 2nd ed.; Princeton University Press: Princeton, NJ, 2008.
(12) O'Faolain, L.; Kotlyar, M. V.; Tripathi, N.; Wilson, R.; Krauss, T. F. *J. Vac. Sci. Technol., B* **2006**, *24*, 336–339.
(13) Romanato, F.; Businaro, L.; Di Fabrizio, E.; Passaseo, A.; De Vittorio, M.; Cingolani, R.; Patrini, M.; Galli, M.; Bajoni, D.; Andreani, L. C.; Giacometti, F.; Gentili, M.; Peyrade, D.; Chen, Y. *Nanotechnology* **2002**, *13*, 644–652.
(14) Belotti, M.; Galli, M.; Bajoni, D.; Andreani, L. C.; Guizzetti, G.; Decanini, D.; Chen, Y. *Microelectron. Eng.* **2004**, *73*, 405–411.
(15) Whaley, S. R.; English, D. S.; Hu, E. L.; Barbara, P. F.; Belcher, M. A. *Nature* **2000**, *405*, 665–668.
(16) Estephan, E.; Larroque, C.; Cuisinier, F. J. G.; Balint, Z.; Gergely, C. *J. Phys. Chem. B* **2008**, *112*, 8799–8805.
(17) Lee, W. S.; Mao, C.; Flynn, C. E.; Belcher, A. M. *Science* **2002**, *296*, 892–895.
(18) Mao, C.; Flynn, C. E.; Hayhurst, A.; Sweeney, R.; Qi, J; Georgiou, G.; Iverson, B.; Belcher, A. M. *Proc. Natl. Acad. Sci. U.S.A.* **2003**, *100*, 6946–6951.
(19) Naik, R. R.; Brott, L.; Carlson, S. J.; Stone, M. O. *J. Nanosci. Nanotechnol.* **2002**, *2*, 95–100.
(20) Naik, R. R.; Stringer, S. J.; Agarwal, G.; Jones, S. E.; Stone, M. O. *Nat. Mater.* **2002**, *1*, 169–172.

CA). Images were taken in tapping mode using silicon, rectangular cantilevers (Olympus Microcantilever, OMCL-AC240TS); topography and phase images were taken with 512 × 512 point scans at 1 Hz scan rate, but only the topography images are reported. We always performed several scans over a given surface area assuring reproducible images.

Scanning Electron Microscopy and Energy Dispersive X-ray Spectroscopy. Scanning electron micrographs were taken using a field emission imaging Quante 200 SEM with 15 kV field emission source. The cross-sectional image of the functionalized and naked photonic structure has been taken with different magnification. The EDX analysis was performed with the modified and the unmodified photonic crystal samples.

Linear and Nonlinear Optical Techniques. Linear reflection spectra of the bare and functionalized photonic structures have been measured by means of a Fourier transform spectrometer at variable incidence angles.

The nonlinear properties of the samples involved in the experiments were investigated using ≈130 fs tunable laser pulses generated by an optical parametric oscillator (OPO) in the 1.5 μm range. The laser pulses are focused onto the surface of the sample with a beam spot of ≈30 μm in diameter at a repetition rate of 80 MHz. Control of the intensity of the laser beam is achieved by a combination of a linear polarizer and a half-wave plate. The average power on target is 200 μW. The experimental setup consists of a numerically controlled goniometric system to orient the sample in angle of incidence (θ) and in azimuth (ϕ). Angle resolved detection of the second harmonic signal is achieved through an optical fiber coupling the reflected beam into a photomultiplier. The experimental setup is fully described elsewhere.[21]

Results and Discussion

Design of the Photonic Structure. The challenge in detecting adsorbed molecules is to maximize the optical response of the substrate to the small surface changes induced by the presence of these molecules. To this purpose, photonic crystal waveguides offer several possibilities. The planar structure assures confinement of radiation in plane of the waveguide, granting long interaction lengths between the electromagnetic modes and the surface of the sample.[22,23] Quasi-guided modes in the structure can be designed in such a way as to obtain dispersive resonant features in reflection.[22,23] The corresponding position in energy and momentum is determined by the design parameters of the structure. Moreover it can be expected that the deposition of monolayers of molecules over the entire surface would modify the air-filling factor and the dielectric contrast thus affecting spectral shapes of the optical resonant features and providing specific signatures of the presence of adsorbed compounds. A second possibility is the observation that enhanced sensitivity to the surface conditions may come from the harmonic response of the waveguide PhC structures that are known to exhibit strong enhancements with respect to bulk crystals in correspondence of the modal structures of waveguides[24] and PhC patterned structures.[25−27]

For a proof-of-principle attempt a series of numerical tests were therefore undertaken. A simple asymmetrical air/GaAs/AlGaAs 1D design built on top of a GaAs substrate has been simulated. We have selected the waveguide parameters in order to obtain the radiative PhC resonant features at $\lambda \approx 1.5$ μm at reasonable angles of incidence. The reflectance spectra for transverse electric (TE) and transverse magnetic (TM) polarizations have been simulated with the Fourier modal method, in which Maxwell equations are solved in each layer on a plane wave basis, and the multilayer structure is taken into account using the scattering matrix method.[28] The final design, 600 nm GaAs/1400 nm $Al_{0.6}Ga_{0.4}As$ with variable 1D periodicity between 600 and 700 nm and air trenches of increasing width has been implemented. Figure 1 shows the design of the structure, an example of SEM picture of the fabricated specimen and simulated reflectance spectra for TE and TM polarization. The size of the resonant structure was typically 100 × 100 μm^2. The simulations exhibit sharp and well-resolved resonances, highly visible on the background of interference fringes from the multilayer structure. TE spectra show sharper structures than TM spectra, with line widths of the order of 3−4 nm for TE polarization.

Elaboration of Adhesion Peptides for GaAs. Adhesion peptide with a high affinity for the GaAs semi-insulating substrate was elaborated using the phage display technique described in the experimental section. This affinity selection method is a frequently used technique to select adhesion peptides against a target surface. It consists in successive biopanning rounds when the substrate is incubated in a primary phage library, then rinsing the unbound phages from the target, the adsorbed ones are eluted and then amplified.[29] The obtained secondary library, in its turn, is exposed to the target, and the cycle is repeated leading to a library which is gradually enriched with specific phages. After several biopanning rounds monoclonal phage populations are obtained carrying the genotype of the adhesion peptide presenting binding capacity for GaAs. Once isolated, the DNA sequence encoding them can be determined, and the specific peptide can be synthesized. In our case after three biopanning rounds 10 phages were exported, their DNA extracted and sequenced as they define the genetic code of the adhesion peptides. Three 12 mer-peptides (composed of 12 aminoacids) were expressed: the SVSVGMKPSPRP (P1), NHNTSTWAAYST, and TLPSPHSLLTVH, but 8 over the 10 selected present the same P1 sequence. Thus the P1 peptide was chosen to be the one which presents the best affinity for the GaAs. We note the abundance of its sequence in proline (P) that imprints a high structural constraint to the peptide and thus facilitates adhesion to the surface This phage expressing this P1 peptide was previously isolated and extracted on different targets too.[16,30−36]

(21) Malvezzi, A. M.; Vecchi, G.; Patrini, M.; Guizzetti, G.; Andreani, L. C.; Romanato, F.; Businaro, L.; Di Fabrizio, E.; Passaseo, A.; De Vittorio, M. *Phys. Rev. B* **2003**, *68*, 1–4.
(22) Galli, M.; Bajoni, D.; Belotti, M.; Paleari, F.; Patrini, M.; Guizzetti, G.; Gerace, D.; Agio, A.; Andreani, L. C.; Peyrade, D.; Chen, Y. *IEEE J.Sel. Areas Commun.* **2005**, *23*, 1402–1410.
(23) Andreani, L. C. *Phys. Status Solidi B* **2002**, *234*, 139–146.
(24) Comaschi, C.; Vecchi, G.; Malvezzi, A. M.; Patrini, M.; Guizzetti, G.; Liscidini, M.; Andreani, L. C.; Peyrade, D.; Chen, Y. *Appl. Phys. B: Laser Opt.* **2005**, *81*, 305–312.
(25) Vecchi, G .; Torres, J.; Coquillat, D.; Le Vassor d'Yerville, M.; Malvezzi, A. M. *Appl. Phys. Lett.* **2004**, *84*, 1245–1247.
(26) Torres, J.; Coquillat, D.; Le Vassor d'Yerville, M.; Centeno, E.; Albert, J. P. *Phys. Rev. B* **2005**, *71*, 195326.
(27) Coquillat, D.; Vecchi, G .; Comaschi, C.; Malvezzi, A. M.; Le Vassor d'Yerville, M.; Coquillat, D.; Vecchi, G.; Comaschi, C.; Malvezzi, A. M.; Torres, J.; Le Vassor d'Yerville, M. *Appl. Phys. Lett.* **2004**, *87*, 101106.
(28) Whittaker, D. M.; Culshaw, I. S. *Phys. Rev. B* **1999**, *60*, 2610–2618.
(29) Willats, W. G. T. *Plant Mol. Biol.* **2002**, *50*, 837–854.
(30) Kolb, G.; Boiziau, C. *RNA Biol.* **2005**, *2*, e2–e7.
(31) Arnaiz, B.; Madrigal-Estebas, L.; Todryk, S.; James, T. C.; Doherty, D. G.; Bond, U. A *J. Immune Based Ther. Vaccines* **2006**, *4*, 1–12.
(32) Hou, S. T.; Dove, M.; Anderson, E.; Zhang, J.; Mackenzie, C. R. *J. Neurosci. Methods* **2004**, *138*, 39–44.
(33) Tamler, C.; Sarikaya, M. *Acta Biomater.* **2007**, *3*, 289–299.
(34) Wiesehan, K.; Buder, K.; Linke, R. P.; Patt, S.; Stoldt, M.; Unger, E.; Schmitt, B.; Bucci, E.; Willbold, D. *Chembiochem* **2003**, *4*, 748–753.
(35) Estephan, E.; Saab, M. B.; Larroque, C.; Martin, M.; Olsson, F.; Lourdudoss, S.; Gergely, C. *J. Colloid Interface Sci.* **2009**, *337*, 358–363.
(36) Estephan, E.; Larroque, C.; Bec, N.; Martineau, P.; Cuisinier, F. J. G.; Cloitre, T.; Gergely, C. *Biotechnol. Bioeng.* **2009**, *104*, 1121–1131.

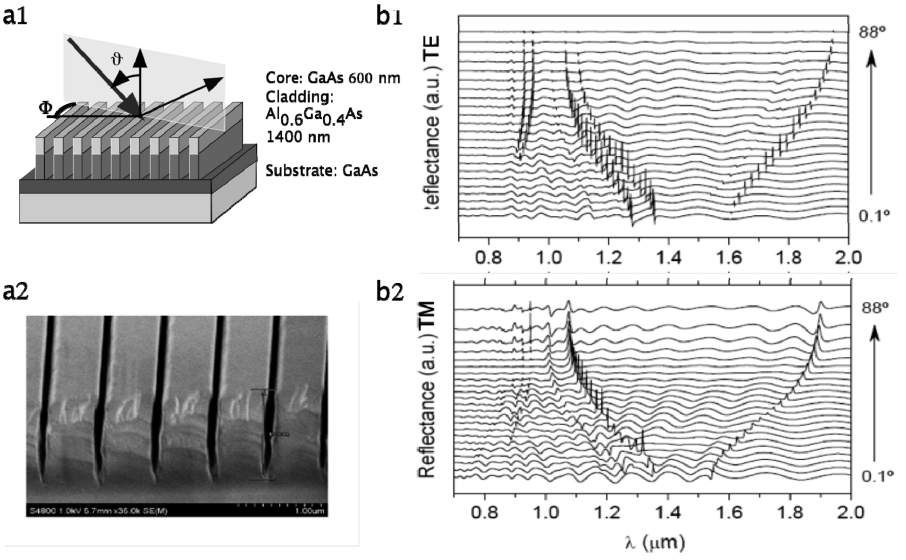

Figure 1. (a1) Scheme of the photonic crystal structure and geometry of the experiment with angle of incidence θ and azimuth angle ϕ shown; (a2) SEM image of the etched sample; (b1) calculated reflectance spectra for TE; and (b2) TM polarization as function of wavelength and angle of incidence. Traces refer to the range of incidence angles shown on the right and are shifted vertically for clarity.

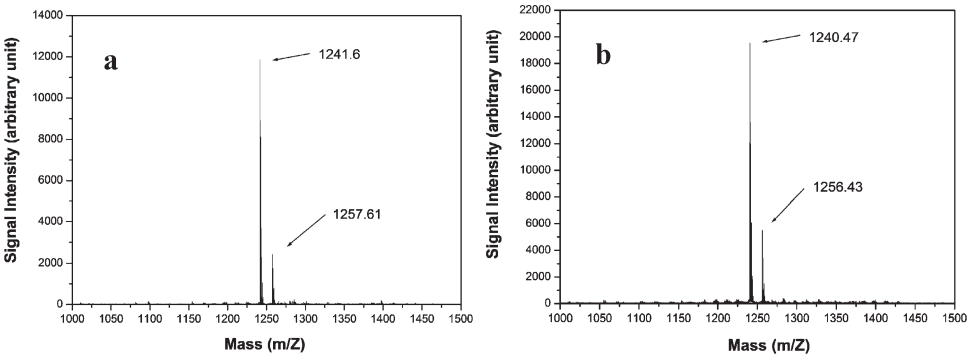

Figure 2. Mass (MALDI MS) spectra (a) of the single peptide adsorbed on the Maldi plate and (b) of the functionalized GaAs surface. The difference in the measured mass (-1.15 ± 0.03) for the P1 peptide over the two conditions is due to a modification in the MALDI ionization cavity induced by the introduction of the semiconductor sample.

To verify its real capacity to bind to the GaAs target, mass spectrometry (MALDI−TOF/TOF) has been employed. As reference the spectrum of the single P1 peptide was first recorded.

The spectrum in Figure 2a reveals the mass of 1241.6 $[M+H]^+$ corresponding to the theoretical mass of the peptide. A second spectral line of smaller intensity at 1257.6 is also present that is derived from the oxidation of the methionine (M) present in the peptide sequence $[M+O+H]^+$. The corresponding mass spectrum of the functionalized GaAs reveals a peak at 1240.47 ($\delta = -1.13$) and a peak at 1256.43 (Figure 2b), demonstrating the presence of P1 and of the oxidized P1 on the surface, despite that the surface was thoroughly rinsed with deionized water. Hence the P1 peptide is indeed presenting a high binding capacity for the GaAs surface, and it will be used for further functionalization.

Biofunctionalization of the GaAs/AlGaAs Photonic Crystal. Before being used for sensing streptavidin the photonic structure was first functionalized via biotin molecules linked to the P1 peptide revealing affinity for the GaAs and then used. To obtain the biotinilated peptide, a short flexible and stable GGGSK sequence has been added at the P1 peptide C-terminus, and then biotin was linked to the terminal lysine. The previously deoxidized GaAs/AlGaAs structure was incubated in the biotinilated P1 peptide, left to adsorb, then thoroughly rinsed to remove unbound and excess peptide. The photonic structure was then immersed in 50 μM streptavidin (in BSA 1% −PBS solution) left to adsorb for 1 h, then rinsed with deionized water in order to remove excess and unbound streptavidin and salt traces. Drying with nitrogen can be performed after each step for experimental needs.

For controlling the morphological status of the functionalized photonic crystal, atomic force microscopy was employed. First the image of the bare photonic crystal, before functionalization, was recorded in air and tapping mode (Figure 3a), revealing a rather smooth GaAs surface. The depth of the air-stripes was in the range of 80−125 nm as measured with rectangular cantilevers of very small tip radius curvature (< 10 nm) for high lateral resolution and accuracy.

The AFM images of the photonic structure fully modified with the peptide-biotin and streptavidin reveal the molecules adsorbed into an almost complete surface coverage (Figure 3b). The section analysis reveals a rougher surface compared to that of the bare sample, but roughness is never exceeding 10 nm suggesting the formation of a molecular monolayer without any aggregation on the top of the GaAs. This strengthens the value of our novel specific functionalization via GaAs recognizing peptides in avoiding unwanted aggregation of molecules that often leads to a decrease in precision in detection. Moreover, our AFM images suggest that the biomolecules were successfully infiltrated into the

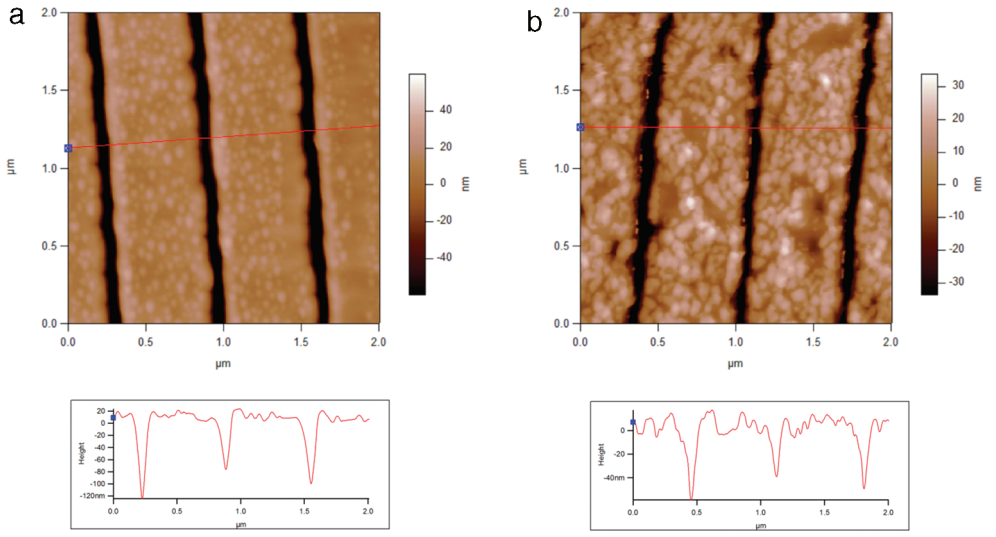

Figure 3. AFM micrographs and section analysis (a) of the bare photonic crystal and (b) of the functionalized photonic crystal after streptavidin capture.

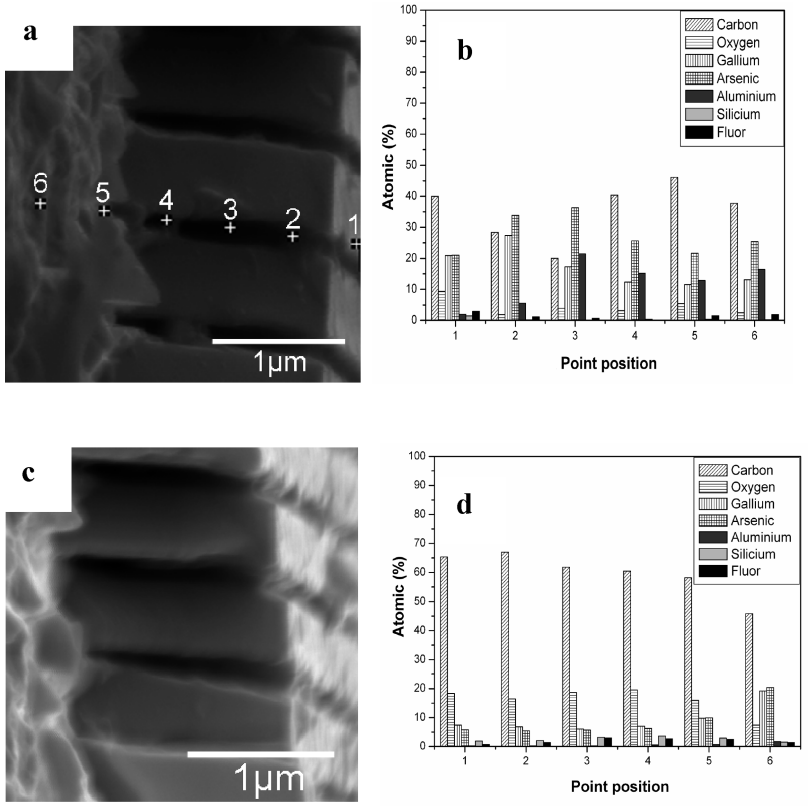

Figure 4. (a, b) SEM images (section view) and EDX analyses of the unmodified photonic crystal. (c, d) SEM images and EDX analyses of the functionalized photonic crystal after streptavidin capture.

structure and adsorbed also onto the inner walls of the structure, as the apparent depth of the air stripes as measured by AFM decreased to 40−60 nm when the peptide-biotin and streptavidin molecules were adsorbed onto the PhC.

Achieving penetration of molecules in such tiny (100 × 100 μm^2) devices, through ~100 nm narrow slots is not evident, thus functionalization and penetration of biomolecules into the photonic crystal was monitored by cross-sectional scanning electron microscopy (SEM) and coupled energy dispersive X-ray (EDX) analysis. The SEM images (Figure 4a,c) and the corresponding EDX profiles (Figure 4b,d) along the crystal structure (in 6 points) were recorded for both the functionalized and the naked samples, the latter serving as a reference.

The elements characteristic for the used material as Ga, As, and Al have been found by the EDX measurements as well as some traces of Si coming from the HSQ mask used for lithography (Figure 4b,d). Some F is present too that we allocate to remaining traces of the etching process. The source of carbon (C) and oxygen (O) found in the EDX spectra of the bare sample is coming from surface contamination by the ambient air which contains CO, CO_2, and hydrocarbon molecules. The significant increase in the

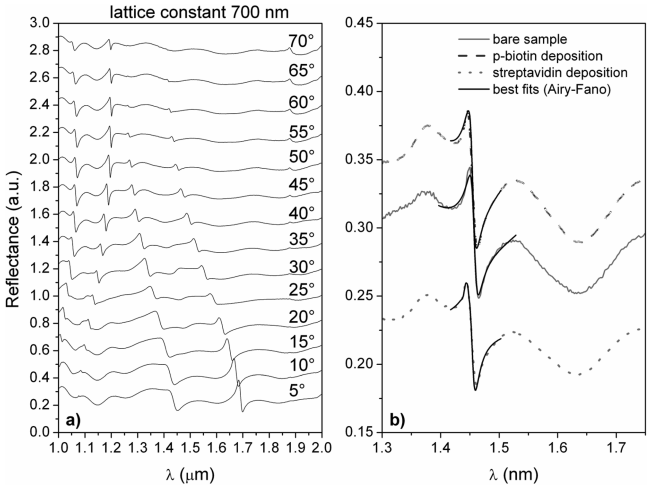

Figure 5. (a) Angle-resolved reflectance spectra (TE polarization) for a PhC with 700 nm lattice constant in the 1−2 μm wavelength range. The various spectra refer to the angles of incidence shown. The curves are shifted vertically for better comparison. (b) Reflectance at 40° for a sample with a lattice constant of 690 nm before and after functionalization. The continuous bold lines are the best-fits using the Fano model.

atomic percentage of carbon and oxygen in the functionalized sample (Figure 4d) proves the penetration of organic molecules along the entire photonic structure, within a depth of about 2 μm. These data constitute the first report, to the best of our knowledge, on successful wetting and molecular infiltration of miniaturized photonic nanostructures.

Optical Sensing of Molecules. The linear optical properties of the PhC waveguide have been investigated by angle-resolved reflectance as shown in Figure 5a.

The spectra show photonic structures in good agreement with the simulations. In particular, a strong resonant feature in the 1.5−1.6 μm range (i.e., the tuning range of the laser pump in the nonlinear experiments) is observed at angles of incidence between 25 and 40 degrees, as expected. The same reflectance spectra were then recorded after functionalization with biotinilated peptide and capture of streptavidin. The results are shown in Figure 5b. No difference in spectral features or in intensity of the reflected signal is detectable after the functionalization. This result is in line with the surface coverage of the samples that is observed to be of the order of one monolayer, that is, too thin to induce index-related changes in the photonic band structure. To quantitatively confirm this observation we have fitted the experimental data using Fano lineshapes[37] as shown in Figure 5b: the fits yield the same values for the resonance wavelength and width in all the three cases.

Second harmonic generation (SHG) from the patterned waveguide has been attempted next using the apparatus described in the Materials and Methods section. In general, SHG is observable in reflection from absorbing materials at high laser pump intensities, and its occurrence is determined by the symmetry of the material and by the surface.[38] The latter contribution can become higher than the former when specific molecular resonances with laser frequency are present in the adsorbed molecules or when the surface structure determines resonances in the modal structure of the propagating radiation.[24] SHG can also be simply enhanced by the roughening of the interface due to presence of adsorbed

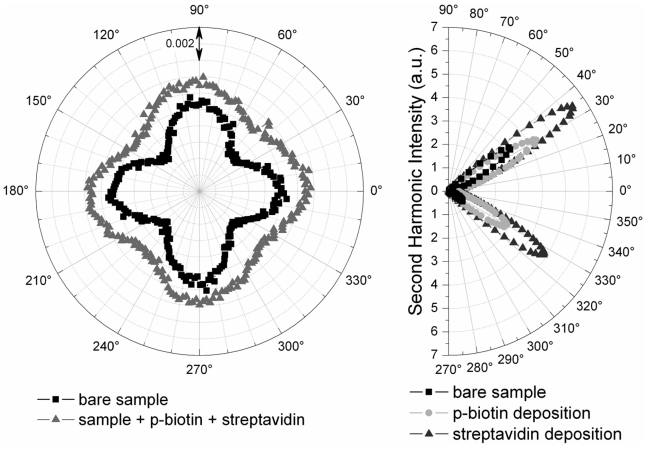

Figure 6. (a) Polar diagram of the second harmonic signal detected as a function of the azimuth angle ϕ in reflection from the unpatterned bare sample before (squares) and after functionalization with biotinilated peptide and streptavidin (triangles). The laser wavelength is 1550 nm, angle of incidence is 40 degrees, spot diameter is 30 μm, and average power on sample is 200 μW. (b) Second harmonic signal in reflection vs azimuth sample rotation ϕ generated by the photonic structure. Squares refer to untreated surface, dots to peptide-biotinilated surface, and triangles to the capture of streptavidin. $\phi = 0$ corresponds to the plane of incidence perpendicular to air stripes on the PhC surface. Note that in both diagrams units, although arbitrary, are congruent.

molecules.[39] The data presented in Figure 6a illustrate this last point for the SH reflected signal on unpatterned bare samples and on those biotinilated and treated with streptadivin in a polar SH diagram. The well-known 4-fold symmetry emission of the bare GaAs surface[21,40] is observed before functionalization. When the sample is covered with streptavidin an isotropic increase of the SH signal is observed indicating an optical nonlinear response of the surface molecules superimposed to the bulk response of the sample. These data are consistent with the picture of an enhanced SH signal almost dominating the bulk response of GaAs and determined solely by the presence of the proteins adsorbed at the sample surface. Note that pump and SHG frequencies are not resonant with any of the adsorbed molecules. This is one of the reasons why SHG spectroscopy has been previously employed as an intrinsically surface-selective technique to discriminate between surface-bound and free molecules.[41]

The same measurements have been repeated onto the patterned area of the sample (see Figure 6b). The SH signal is greatly enhanced and emitted into two narrow lobes symmetrically located around the direction of symmetry of the 1D photonic waveguide. The photonic structure dominates completely the SH pattern[42] and no sign of crystal symmetry is apparent anymore. The angular position of the lobes is determined by (a) the shape of the resonant photonic band at the fundamental laser frequency that is symmetric with respect to plane $\phi = 0$; (b) the energy conservation, $E_{SHG} = 2E_{pump}$; (c) the momentum conservation, that is, $2k^{\parallel}_{in}(\omega) = k^{\parallel}_{out}(2\omega)$ for the in-plane components of wavevector **k**.[41,43] All these factors concur in increasing substantially the level of SH generation and in providing a higher SH intensity ratio for fully modified and bare PhC, hence a better contrast compared to the unstructured surface. An estimate of the

(37) Fano, U. *Phys. Rev.* **1961**, *124*, 1866–1878.
(38) Brown, F.; Matsuoka, M. *Phys. Rev.* **1969**, *185*, 985–987.
(39) Shen, Y. R. *IEEE J. Sel. Top. Quant.* **2000**, *6*, 1375–1379.
(40) Malvezzi, A. M.; Cattaneo, F.; Vecchi, G.; Falasconi, M.; Guizzetti, G.; Andreani, L. C.; Romanato, F.; Businaro, L.; Di Fabrizio, E.; Passaseo, A.; De Vittorio, M. *J. Opt. Soc. Am., B* **2002**, *19*, 2122–2128.
(41) Salafsky, J. S.; Eisenthal, K. B. *J. Phys. Chem. B* **2000**, *104*, 7752–7755.
(42) Cowan, A. R.; Young, J. F. *Phys. Rev. B* **2002**, *65*, 1–6.
(43) Freund, I. *Phys. Rev. Lett.* **1968**, *21*, 1404–1406.

maximum SHG intensity detected falls in the 2×10^2 W/m^2 range. Therefore the estimated nonlinear reflectivities are in our case in the 4×10^{-19} W/m^2. These figures are consistent with bulk GaAs nonlinear reflectivity and a Q-factor equal to 100 obtained from Fano fitting the resonant features in linear reflectance of Figure 5b. The ratio of SH signal with streptavidin coverage to that of the bare sample in Figure 6b provides the enhancement factor before and after the functionalization. The values are ~2 and ~7 for the upper and lower lobes, respectively. They are to be compared with the corresponding values for the unpatterned surface of Figure 6a ranging between 1.2 and 1.7. In essence the quasi-guided modes of the photonic crystal enhance the efficiency of the second harmonic generation from the adsorbed molecules,[21] resulting in more sensitive discrimination capabilities.

The fact that the measured SH lobes keep almost the same form after protein capturing indicates that the adsorbed molecules do not disturb the nonlinear response of the PhC. This strengthens the crucial role of our novel functionalization method, through nanometer-sized adhesion peptides, leading to molecular monolayers onto the PhC (shown in the AFM images). It is assumed that some order in the peptide-biotin monolayers renders them more available to capture streptavidin for an efficient sensing by SHG.

The observed signal enhancement allows the detection of molecules even for concentrations to which linear optical techniques are insensitive as discussed above. It is interesting to estimate the number of streptavidin molecules contributing to the nonlinear signal. Assuming a monolayer coverage of the surface and of the walls of the trenches illuminated by the 30 μm laser spot, the result gives an upper limit of ~10^8 molecules or 0.16 fmoles that are contributing to the nonlinear signal. Monitoring the second harmonic signal proved to be highly sensitive for detecting molecules at low quantities where linear optics failed to be efficient. Interferometric sensing approaches generally offer nanomolar sensitivities as described for porous silicon microcavity structures.[44,45] Recently molecular detection at zeptomole sensitivity has been reported via the resonant coupling of plasmonic modes of split ring resonators and infrared vibrational modes of octadecanthiol molecules.[3] The obtained remarkable sensitivity is due to the extremely small size of the gap surface area of a single nanoresonator, but the method lacks specificity that sensing based on infrared vibrational modes cannot offer. The sensitivity of our approach is limited by the micrometer-sized laser spot size, but it offers affinity based sensing, that is, specific molecular (streptavidin) recognition via the peptide-biotinilized photonic crystals.

(44) Palestino, G.; Legros, R.; Agarwal, V.; Perez, E.; Gergely, C. *Sens. Actuators, B* **2008**, *135*, 27–34.
(45) Martin, M.; Palestino, G.; Agarwal, V.; Cloitre, T.; Zimányi, L.; Gergely, C. *Appl. Phys. Lett*. **2009**, *94*, 223313-1-3.

Conclusions

Peptides revealing high binding capacity for GaAs have been produced by means of phage display technology, and its adhesion and real affinity toward GaAs has been demonstrated by MALDI-TOF/TOF mass-spectrometry. The specific adhesion of these peptides is used for biofunctionalization of GaAs/AlGaAs photonic waveguides capable of enhancing the second harmonic generation response. Infiltration of biomolecules within these tiny nanostructures has been demonstrated by atomic force microscopy and scanning electron microscopy combined with EDX spectroscopy. The biotinylated-peptides adsorbed on the substrate served to capture streptavidin, and molecular detection was performed by means of nonlinear optical response of the structure. Our work describes thus a proof-of-concept new procedure for sensing molecules by nonlinear optics. We have achieved a novel device for biosensing applications composed by (i) the sensitive biological element created by biological engineering (biotinilated peptide recognizing the GaAs) and (ii) the transducer (the photonic crystal) that transforms the signal resulting from the interaction of the sensitive biological element with the target molecule (streptavidin) into a nonlinear optical signal that can be measured and quantified. Our results prove the outstanding sensitivity of the obtained miniaturized biosensor: nonlinear optics detects molecules at concentrations where linear optics fails.

Use of nanostructured photonic crystal waveguides with large sensing surface accurately functionalized for specific binding of biomolecules opens up the way for a new class of miniaturized affinity-based biosensors functioning on signal enhancement due to nonlinear optical effects.

Acknowledgment. This work was supported by the Phoremost European Network of Excellence, Project No. 511616: "NanoPhotonics to Realize Molecular Scale Technologies" and by the COST−EU Action MP0702: "Towards functional sub-wavelength photonic structures". We thank René Legros from the UMR5650-CNRS University Montpellier 2 for kindly supplying the substrate and William Whelan-Curtin from St. Andrews, U.K. for his help in the fabrication of the photonic structures. Fruitful comments and discussions with Maddalena Patrini and Matteo Galli are also gratefully acknowledged.